

Review

The Linac Coherent Light Source: Recent Developments and Future Plans

R. W. Schoenlein *, S. Boutet, M. P. Minitti and A.M. Dunne

SLAC National Accelerator Laboratory, Linac Coherent Light Source, 2575 Sand Hill Rd, Menlo Par, CA 94025, USA; sboutet@slac.stanford.edu (S.B.); minitti@slac.stanford.edu (M.P.M.); mdunne@slac.stanford.edu (A.M.D.)

* Correspondence: rwschoen@slac.stanford.edu; Tel.: +1-650-926-5155

Received: 31 July 2017; Accepted: 10 August 2017; Published: 18 August 2017

Abstract: The development of X-ray free-electron lasers (XFELs) has launched a new era in X-ray science by providing ultrafast coherent X-ray pulses with a peak brightness that is approximately one billion times higher than previous X-ray sources. The Linac Coherent Light Source (LCLS) facility at the SLAC National Accelerator Laboratory, the world's first hard X-ray FEL, has already demonstrated a tremendous scientific impact across broad areas of science. Here, a few of the more recent representative highlights from LCLS are presented in the areas of atomic, molecular, and optical science; chemistry; condensed matter physics; matter in extreme conditions; and biology. This paper also outlines the near term upgrade (LCLS-II) and motivating science opportunities for ultrafast X-rays in the 0.25–5 keV range at repetition rates up to 1 MHz. Future plans to extend the X-ray energy reach to beyond 13 keV ($<1 \text{ \AA}$) at high repetition rate (LCLS-II-HE) are envisioned, motivated by compelling new science of structural dynamics at the atomic scale.

Keywords: ultrafast; X-ray; XFEL; X-ray free-electron laser

1. Introduction

A new era in X-ray science has been launched by the development of X-ray free-electron lasers (XFELs) which provide ultrafast coherent X-ray pulses with a peak brightness that is approximately one billion times higher than previous X-ray sources. The FLASH facility at DESY in Hamburg (the first extreme ultraviolet XFEL) [1], the LCLS facility at SLAC National Accelerator Laboratory (the first hard X-ray XFEL) and the SACLA facility in Japan [2] represent the first generation of XFEL sources, and they have already demonstrated the tremendous scientific potential and impact across broad areas of science.

A comprehensive overview of the scientific impact of the first five years of operation of LCLS was published in *Reviews of Modern Physics* in 2016 [3]. This paper will highlight some of the more recent accomplishments from LCLS in the areas of atomic, molecular, and optical science; chemistry; condensed matter physics; matter in extreme conditions; and biology. This paper also presents an outline of the upgrade plans for the facility along with the motivating science opportunities. In particular, LCLS is now in the middle of an upgrade project (LCLS-II) which will provide ultrafast X-rays in the 0.25 keV–5 keV range at repetition rates up to 1 MHz with two independent XFELs based on adjustable-gap undulators: 0.25 keV–1.25 keV soft X-ray undulator (SXU) and 1 keV–5 keV hard X-ray undulator (HXU) [4]. LCLS-II is based on a new continuous-wave radio-frequency superconducting accelerator (CW-SCRF) operating at 4 GeV, and first-light is projected for 2020. A second phase upgrade is envisioned to extend the X-ray energy reach to beyond 13 keV ($<1 \text{ \AA}$) at a high repetition rate by doubling the CW-SCRF linac energy to 8 GeV. This is motivated by compelling new science of structural dynamics at the atomic scale.

2. LCLS Recent Representative Highlights

Following are some representative recent highlights that illustrate the breadth and depth of LCLS science. These pioneering results are expected to open new areas of science enabled by the unique capabilities of LCLS.

2.1. Gase-Phase Atomic, Molecular, and Optical Science

Ultrafast X-ray pulses from LCLS have revealed for the first time the atomic motions associated with an ultrafast chemical reaction triggered by light, as shown in Figure 1 [5]. The ring opening reaction of 1,3-cyclohexadiene (CHD) to form the linear 1,3,5-hexatriene molecule is a prototypical example of a class of organic electrocyclic reactions [6] that are relevant for a wide range of synthetic chemical processes, photochemical switches, and natural biochemical production. Time-resolved hard X-ray scattering studies at LCLS mapped the structural dynamics by providing snapshots roughly every 25 fs (over the 200 fs lifetime) following initiation of the reaction via ultrafast UV excitation. This time-resolved observation of an evolving photochemical reaction paves the way for a wide range of X-ray studies examining gas phase chemistry and the structural dynamics associated with chemical reactions.

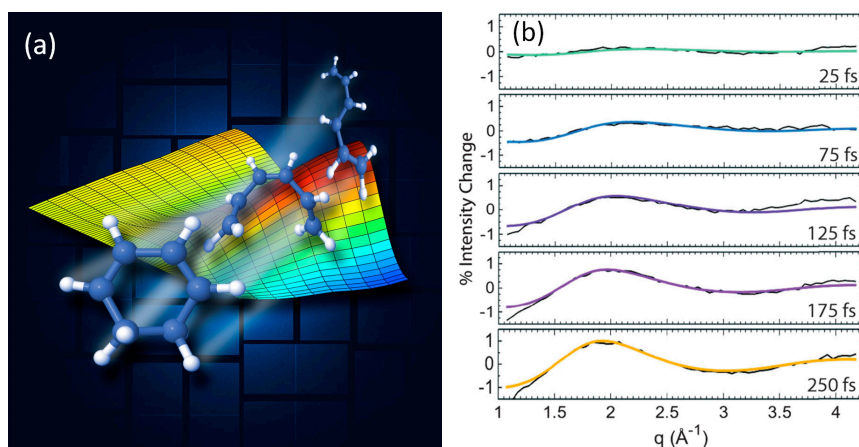


Figure 1. (a) Illustration of femtosecond electrocyclic ring opening of 1,3-cyclohexadiene. (b) Transient X-ray scattering data at a sequence of time delays following initiation of the reaction by an ultrafast UV laser pulse. Reprinted figure with permission from [5]. Copyright The American Physical Society, 2017.

2.2. Condensed-Phase Chemistry

Transition-metal complexes catalyze many important reactions, and their performance is coupled to charge and spin density changes at the metal site caused by electronic excitation and/or ligand loss from the metal center. LCLS results (Figure 2) show that femtosecond X-ray spectroscopy and quantum chemistry theory can provide an unprecedented molecular-level insight into the dynamics of the model transition-metal complex $\text{Fe}(\text{CO})_5$, revealing that light-induced dissociation creates a previously unreported excited singlet species and its subsequent reactions [7]. Time-resolved resonant inelastic X-ray scattering (RIXS) spectroscopy is a powerful tool for mapping the evolution of frontier-orbitals with element-specificity and is expected to be applicable to a wide range of molecular dynamics (and a major area of science for LCLS-II). RIXS probing of electronic structural dynamics complements X-ray scattering approaches that probe the atomic structural changes associated with ultrafast chemical reactions.

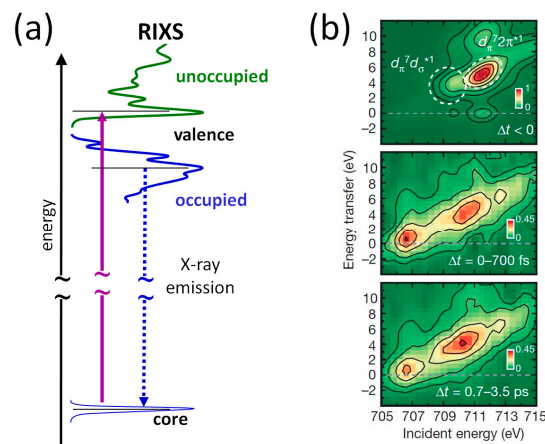


Figure 2. (a) Resonant inelastic X-ray scattering (RIXS) is an element-specific probe of occupied and unoccupied valence states in molecules. (b) Measured Fe L_3 -RIXS intensity maps for $\text{Fe}(\text{CO})_5$ ground-state (top); and difference intensities for the time intervals 0–700 fs (middle) and 0.7–3.5 ps (bottom). Reprinted with permission from [7]. Copyright Nature Publishing Group, 2015.

2.3. Materials Physics

Ultrafast X-ray scattering studies at LCLS resolved for the first time the mechanism responsible for the incipient ferroelectric behavior in the bulk thermoelectric PbTe (Figure 3), and demonstrate the critical importance of electron-phonon interactions [8]. In PbTe and related materials, the ferroelectric instability is associated with thermoelectricity, phase-change behavior, and superconductivity. However, the origin of the instability has long been controversial. Recent studies have focused on the role of anharmonic phonon-phonon interactions in these materials, while largely overlooking the role of electron-phonon coupling. LCLS studies, using the novel approach of Fourier-transform inelastic X-ray scattering (FT-IXS) [9,10], show that ultrafast infrared excitation transiently stabilizes the paraelectric phase, coupling the transverse optical and acoustic phonons propagating along the bonding direction. An important conclusion is that near band-gap electrons preferentially interact with the soft-phonons to induce ferroelectric instability. These results further reconcile the band and bond pictures of ferroelectricity, which has broad implications for broken-symmetry states in materials with strong electron-phonon interactions.

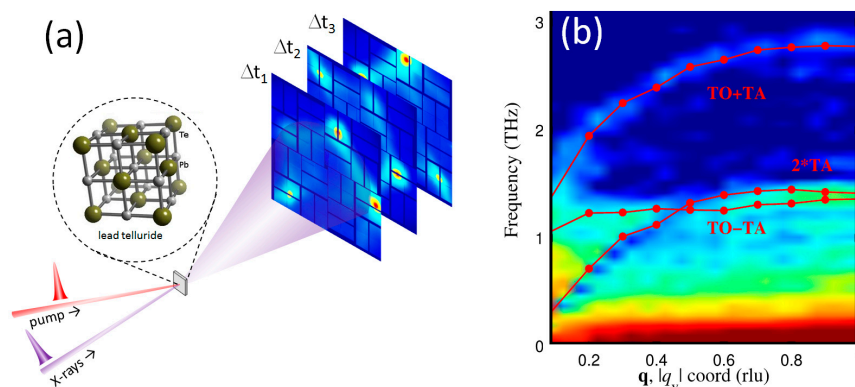


Figure 3. (a) Set-up for time-resolved inelastic X-ray scattering for probing nonequilibrium lattice dynamics. (b) Ultrafast two-phonon spectrum of PbTe obtained through Fourier transform of the femtosecond X-ray scattering signal. The results show a combination of modes (squeezed state) indicative of photo-induced stabilization of the paraelectric state [8].

2.4. Quantum Materials

LCLS provides new insight into quantum materials by enabling transient X-ray scattering studies in the presence of pulsed high magnetic fields. In cuprates and related materials exhibiting unconventional (high- T_c) superconductivity, the universal existence of charge density wave (CDW) correlations raises profound questions regarding the role of CDW phenomena in the emergence of high- T_c superconductivity. Uncovering the evolution of CDW upon suppression of superconductivity by an external magnetic field provides valuable insight into these issues. Studies at LCLS (Figure 4) directly revealed the structure of the long-sought field-induced CDW phase in the high- T_c cuprate $\text{YBa}_2\text{Cu}_3\text{O}_{6.67}$ via time-resolved X-ray scattering in the presence of a transient high magnetic field (28 Tesla) [11]. An unexpected three-dimensionally ordered CDW emerges at low temperatures with magnetic fields above 15 Tesla. This is a distinctly different ordering pattern than that observed previously at zero-field CDW. This discovery of the field-induced CDW provides long-sought information to bridge the gap in cuprate phenomenology, which is critical to uncover the mechanism of high- T_c superconductivity.

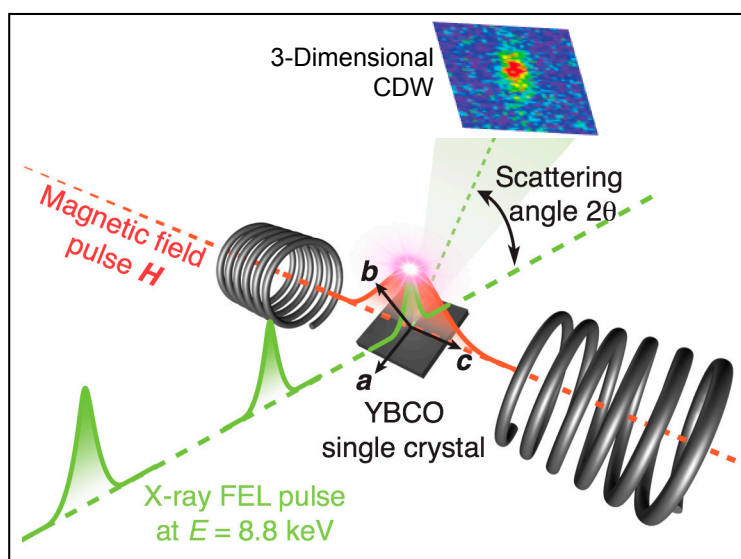


Figure 4. The msec pulsed magnetic field and femtosecond X-ray free-electron laser (FEL) pulses are synchronized to obtain a diffraction pattern from the $\text{YBa}_2\text{Cu}_3\text{O}_{6.67}$ YBCO single crystal at the maximum magnetic field. The 3-dimensional charge density wave (CDW) pattern (inset) was captured with an applied 28 Tesla magnetic field. Reprinted with permission from [11]. Copyright AAAS, 2015.

2.5. Matter in Extreme Conditions

A wealth of new and complex crystal structures emerge from elements exposed to high pressure, an important example of which is the incommensurate composite structure comprised of interpenetrating host and guest components (HG structure) [12]. LCLS shock compression studies (shown in Figure 5) demonstrate for the first time that that these complex crystal structures can develop in less than a few nanoseconds [13]. Time-resolved X-ray scattering studies of scandium under shock compression map the evolving crystal structure along the Hugoniot up to a pressure of 82 GPa. The complex HG crystal structure forms in less than a few nanoseconds, with the guest atoms disordered inside the channels. The onset of melting in scandium is directly observed at the highest compression. This observation of the rapid formation of a complex crystal structure provides an important benchmark of the time scale for atomic rearrangement that is expected to be relevant for a wide range of materials.

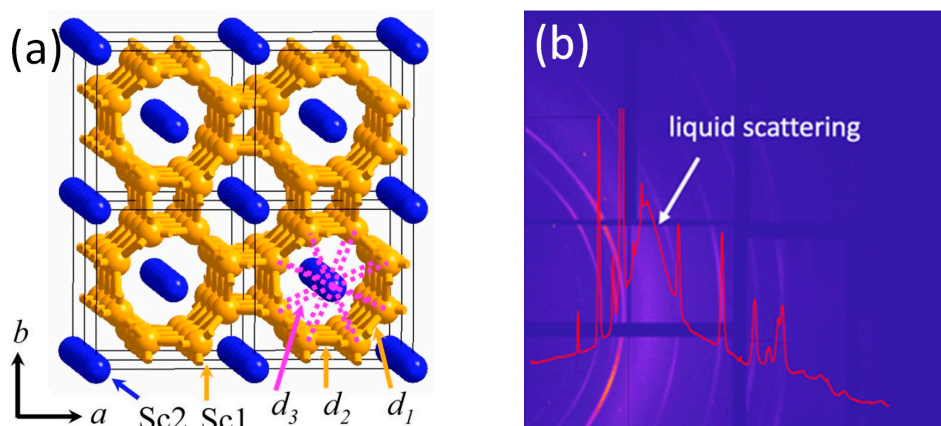


Figure 5. (a) Incommensurate host-guest crystal structure of scandium phase II at 23 GPa. Reprinted with permission from [14]. Copyright The American Physical Society, 2005. (b) Linac Coherent Light Source (LCLS) transient X-ray scattering snapshot of shock-compressed scandium showing liquid scattering (broad diffuse peak) along with uncompressed material ahead of the shockwave (sharp peaks) [13].

2.6. Structural Biology

Serial femtosecond crystallography (SFX) at XFEL sources [1,15–17] has revolutionized the ability to determine macromolecular structures that are inaccessible by synchrotron sources. Furthermore, time-resolved SFX maps the conformational dynamics that determine biological function, and enables studies at room temperature (near physiological conditions).

Recent LCLS time-resolved SFX studies of riboswitches, structural elements of messenger RNA (mRNA), capture the dynamic structural response to the binding of a ligand for the first time, as shown in Figure 6 [18]. This ligand-triggered conformational reaction in mRNA mediates gene expression. By using ultra-small riboswitch crystals, the diffusion of a ligand can be timed to initiate a reaction just prior to X-ray diffraction, thereby capturing the transient structure. Four transient structures identified support a reaction mechanism model with at least four states, and illustrate the structural basis for signal transmission. These results further demonstrate the potential of “mix-and-inject” time-resolved serial crystallography to study important interactions between biological macromolecules and ligands.

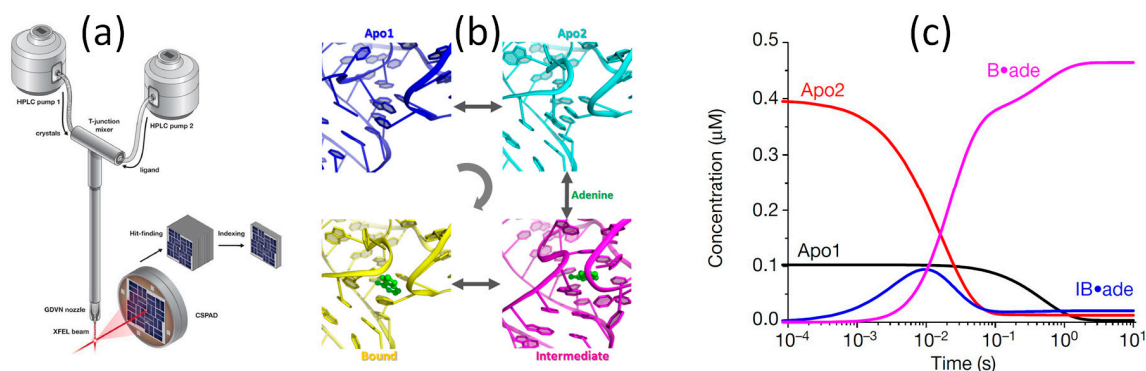


Figure 6. (a) Apparatus for “mix-and-inject” time-resolved serial crystallography at LCLS. (b) Structural snapshots of the binding pocket in the riboswitch viewed from the same angle (figure from Y.-X. Wang of NCI). (c) Evolution of species concentrations over time. Reprinted with permission from [18]. Copyright Nature Publishing Group, 2017.

Room temperature time-resolved SFX studies at LCLS have substantially advanced our understanding of the mechanism underlying sunlight-driven oxidation of water by photosystem II (PS II) [19]. The four-electron redox chemistry of water oxidation is accomplished by the Mn_4CaO_5 cluster in the oxygen-evolving complex (OEC) within PS II. A grand science challenge is to elucidate the transient structures of the OEC in the different chemical transition states, particularly the transient binding of two water molecules at the catalytic site. LCLS SFX studies have captured the transient structures of the OEC in the dark S_1 and illuminated S_3 state at high resolution (2.25 to 3.0 Å), in situ and at room temperature. Substrate water and ammonia (water-analog) binding to the Mn_4Ca catalyst reveal new details about the mechanism of water oxidation.

2.7. XFEL Physics

The development of powerful new XFEL capabilities has been a hallmark of LCLS since its inception. Prominent examples include ultrashort X-ray pulse generation [20,21], self-seeding in both the hard X-ray [22] and soft X-ray ranges [23], and novel approaches for characterizing the X-ray pulse duration [24]. These developments are driven primarily by scientific need and potential impact, and are facilitated by close interaction between X-ray scientists and XFEL physicists at LCLS. At the same time, new XFEL capabilities trigger the development of creative new experimental approaches that enhance the scientific impact of the facility.

Recently, LCLS has developed a novel fresh-slice technique for multicolor XFEL pulse production (Figure 7), wherein different temporal slices of an electron bunch lase to saturation in separate undulator sections [25]. This method combines electron bunch tailoring from a passive wakefield device with trajectory control to provide multicolor pulses. The fresh-slice scheme outperforms existing techniques at soft X-ray wavelengths. It produces femtosecond pulses with a power of tens of gigawatts and flexible color separation. The pulse delay can be varied from temporal overlap to almost one picosecond. We have further demonstrated the first three-color XFEL and variably polarized two-color pulses.

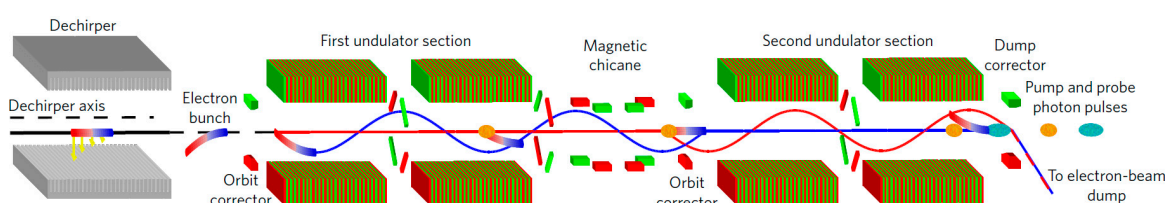


Figure 7. Fresh-slice multi-pulse scheme. The electron bunch propagates off-axis in the dechirper to create a strong transverse head–tail kick. The subsequent oscillating orbit (in combination with fixed-magnet corrections) is exploited so that the tail of the bunch (orange) lases in the first undulator section (at energy E_1) and the head of the bunch (blue) lases in the second undulator section (at energy E_2). The current LCLS layout allows for up to three pulses with controlled photon energies and pulse delays. Reprinted with permission from [25]. Copyright Nature Publishing Group, 2016.

3. LCLS-II Science Opportunities

The representative recent highlights illustrated above are just a glimpse of the remarkable scientific impact achieved by LCLS and related facilities that comprise the first generation of X-ray free-electron lasers. Similar facilities are just beginning operation or are under constructions around the world, including PAL-FEL in the Republic of Korea and Swiss-FEL in Switzerland [26]. However, despite the enormous peak brightness, the average X-ray brightness from this initial generation of XFEL facilities is quite modest, owing to the low repetition rate associated with pulsed-RF accelerator technology. This restricts their impact in many important areas of science that require both high average brightness and ultrafast time resolution.

A new generation of XFELs is now under development that will overcome this limitation by exploiting superconducting RF accelerator technology (SCRf) to provide ultrafast X-ray pulses at

high repetition rate. This development is driven by important new science opportunities that have been identified and advanced over the past decade through scientific workshops around the world. The European-XFEL in Germany is the first of this new generation, spanning the hard and soft X-ray ranges and delivering 10 Hz bursts of 2700 pulses at ~ 4.5 MHz, representing an average repetition rate of up to 27 kHz. Most recently, a series of science workshops held at SLAC National Accelerator Laboratory in 2015 focused on the new science opportunities [27] that will be enabled by the LCLS upgrade project (LCLS-II), based on a novel continuous wave SCRF (CW-SCRF) accelerator technology. As shown in Figure 8, LCLS-II will provide ultrafast X-rays in the 0.25 keV–5 keV range at repetition rates up to 1 MHz with two independent XFELs based on adjustable-gap undulators: soft X-ray undulator (SXU) spanning the range from 0.25 to 1.6 keV, and the hard X-ray undulator (HXU) spanning the range from 1 keV to 5 keV [4].

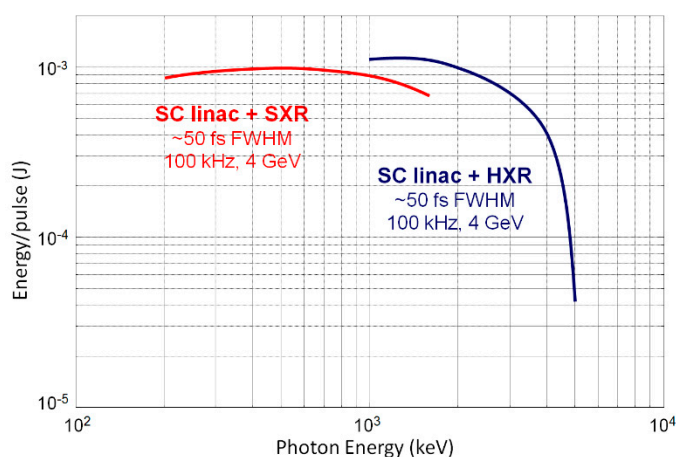


Figure 8. Projected LCLS-II X-ray pulse energies for the soft X-ray undulator (SXU) (red) and the hard X-ray undulator (HXU) (blue) undulators for 100 pC per bunch (from ref. [4]). The X-ray pulse energy is expected to be constant up to ~ 300 kHz, and will scale inversely with repetition rate (i.e., constant average X-ray power) for repetition rates above ~ 300 kHz.

Here we highlight some of the important new science opportunities enabled by such a facility in the areas of (1) fundamental charge and energy flow in molecular complexes; (2) photo-catalysis and coordination chemistry; (3) quantum materials; and (4) coherent imaging at the nanoscale. These examples represent just a few of the many science opportunities where a high repetition rate is particularly enabling, and is not intended to be comprehensive of the broad range of science that is driving the development of such facilities.

3.1. Energy and Charge Dynamics in Atoms and Molecules

The fundamental processes of charge migration, redistribution and localization are at the heart of complex processes such as photosynthesis, catalysis, and bond formation/dissolution that govern all chemical reactions. Such charge dynamics are closely coupled with atomic motion, and substantial evidence points to the importance of the concurrent evolution of electronic and nuclear wave functions (i.e., beyond the Born–Oppenheimer approximation [28]) in many molecular systems. Recent evidence also suggests that quantum coherence in chemical and biological complexes may play a more important role than previously appreciated [29]. Our understanding of these processes at the quantum level is limited, even for simple molecules. We have not been able to directly observe these processes to date, and they are beyond the description of conventional chemistry models.

Ultrafast soft X-rays at a high repetition rate from advanced XFELs will enable new experimental methods that will directly map valence charge distributions and reaction dynamics in the molecular frame. One powerful approach that will be qualitatively advanced by the capabilities of LCLS-II

is the dynamic molecular reaction microscope. As illustrated in Figure 9, the molecular reaction microscope [30–32] employs sophisticated coincidence measurements of photoelectrons (scattered from a molecular structure at the moment of photo absorption) and ion fragments (of the dissociating molecule) to enable a reconstruction of the molecule at a fixed orientation in space. The unique combination of ultrafast X-rays and high repetition rate at LCLS-II will advance these techniques to the time domain to follow molecular dynamics in the excited-state on fundamental time scales. Here specific molecular dynamics are initiated via tailored transient excitations, such as charge transfer, vibrational excitation, the creation of a valence hole via ionization, or the creation of non-equilibrium Rydberg wavepackets.

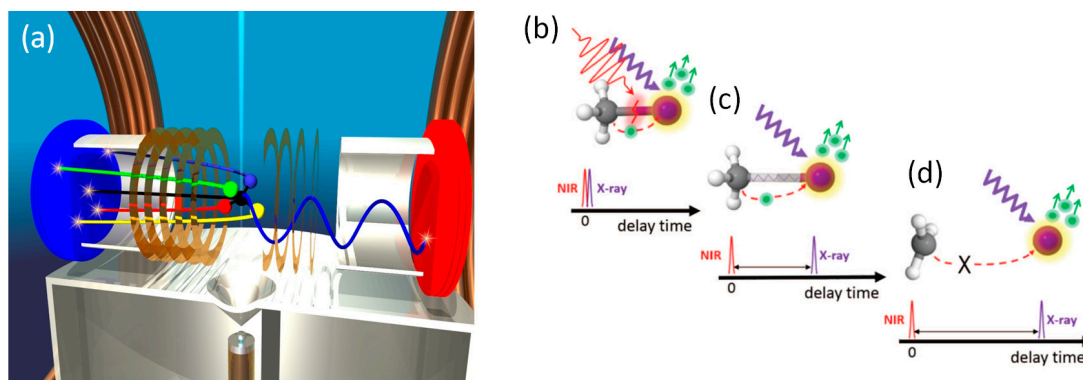


Figure 9. (a) Illustration of a molecular reaction microscope (also known as COLd Target Recoil Ion Momentum Spectroscopy, COLTRIMS). Only one molecule is in the X-ray beam on each pulse (i.e., less than one ionization event per pulse). The electron and ion momenta are fully characterized in coincidence via position-sensitive time-of-flight detectors (graphic courtesy of R. Dörner, Goethe U. Frankfurt). (b–d) Schematic of charge transfer in iodomethane during dissociation. Reprinted with permission from [33]. Copyright AAAS, 2014. Dynamic reaction microscope studies at high repetition rate would enable a full reconstruction of the charge-sharing dynamics in iodomethane and similar complexes in the molecular frame.

Recent experiments highlight the promising opportunities for dynamic reaction microscope studies at high repetition rate XFELs [34–37]. For example, LCLS experiments at 120 Hz by Erk et al. on charge-transfer processes in gas-phase iodomethane [33] identified three dissociative channels based on the time-dependent kinetic energy distributions of the charged fragments (Figure 9 right). Measurements at high repetition rate will enable the complete spatial reconstruction of the excited-state charge transfer and subsequent dissociation of iodomethane at each time step for a particular molecular orientation. The more than 1000-fold increase in coincidence rates (and information content) from LCLS-II will transform this into a powerful approach for visualizing a broad range of ultrafast molecular dynamics from dissociation of simple diatomic molecules, to charge-transfer processes, to isomerization and ring-opening reactions [5], to non-Born–Oppenheimer relaxation processes [38], to quantum symmetry breaking events from which chirality emerges [39].

3.2. Photochemistry and Catalysis

The directed design of photo-catalytic systems for chemical transformation and solar energy conversion (particularly systems that are efficient, chemically selective, robust, and based on earth-abundant elements) remains a major scientific and technological challenge. Meeting this challenge requires a much deeper understanding of the fundamental processes of photo-chemistry that influence the performance of photo-catalysts; namely, stable charge separation, transport, and localization. In molecular systems, these events are mediated by internal conversion, intersystem crossing, and conformational changes on the ultrafast time scale. Understanding such processes

in molecular systems is hindered by the limited ability of conventional experimental or theoretical approaches to directly observe or calculate these charge dynamics. For example, ultrafast optical spectroscopy can capture charge dynamics (and reveal quantum coherences), but is limited to probing electronic states delocalized over multiple atomic sites (or overlapping vibrational spectra), and thus lack element specificity and struggle to identify nuclear degrees of freedom coupled to excited-state dynamics.

Since charge separation, charge transport, and catalysis are local phenomena, the resolving power and element specificity of X-rays can provide insight that is unavailable from non-local probes. Ultrafast X-ray can thus disentangle the coupled motion of electrons and nuclear dynamics, making them uniquely powerful for studying chemical dynamics. High repetition rate X-rays from LCLS-II will enable a powerful suite of spectroscopy tools for understanding the physics and chemistry of photo-catalysts in operating environments. One important example where LCLS-II capabilities will provide a qualitative advance beyond what is presently possible at LCLS is resonant inelastic X-ray scattering (RIXS). As illustrated in Figure 2 RIXS measures the energy distribution of both occupied and unoccupied molecular orbitals, via resonant transitions from a specific atomic core level, thus providing sensitivity to the local chemistry with high resolution.

As highlighted in Section 2.2, recent demonstration experiments at LCLS have applied femtosecond time-resolved RIXS to investigate the charge transfer and ligand exchange dynamics of $\text{Fe}(\text{CO})_5$ in solution [7]. By comparing 2D RIXS maps with quantum chemical calculations, the dynamics of the frontier orbitals and their interactions are revealed for the first time with element specificity. These studies demonstrate the potential of time-resolved RIXS to capture short-lived reaction intermediates and correlate the underlying orbital symmetry with spin multiplicity and reactivity. However, the low repetition rate (and corresponding low average spectral flux: ph/s/meV) of LCLS presently limits the application of time-resolved RIXS to studies of gross structural changes in model molecular systems at high concentrations (e.g., ~1 M in the case of the $\text{Fe}(\text{CO})_5$ studies [7]). With the more than 1000-fold increase in average brightness provided by LCLS-II, time-resolved RIXS with high spectral resolution will enable complete time-sequenced measurements at high fidelity. The resulting detailed mapping of frontier orbital energies and subtle conformational changes will drive a major advance in our understanding of charge separation and transfer in complex functioning systems where the active sites are often in dilute concentrations.

3.3. Quantum Materials

“Quantum materials” are materials where charged particles behave collectively in ways we are unable to predict from the conventional single-electron band models that effectively describe simple metals and semiconductors. For quantum materials, reductionist approaches that consider only individual atoms, electrons and their orbitals are inadequate. Rather, hallmarks of quantum materials are competing or entwined order, phase separation, and heterogeneity (e.g., fluctuating nanoscale texture of charge, spin and orbitals) that result from strong coupling between constituent particles (charge, spin, orbitals, and phonons). These quantum interactions give rise to important “emergent” macroscopic properties such as high-temperature superconductivity, colossal magnetoresistivity, and topologically protected phases.

One fundamental model for understanding the charged collective modes of an interacting electron system is the two-particle dynamic structure factor, $S_e(\mathbf{q},\omega) \sim \chi(\mathbf{q},\omega)$ that describes inter-particle correlations as a function of momentum-transfer (\mathbf{q}) and energy (ω). Although the study of quasiparticles in quantum materials is now well advanced, we still lack effective experimental methods to directly probe $S_e(\mathbf{q},\omega)$ in relevant materials. Because of the subtle balance among competing interactions in quantum materials, the important ground states are determined by collective modes in the 1 to 100 meV energy range as illustrated in Figure 10. In this region, modern X-ray sources and X-ray emission spectrometers struggle to achieve the combination of photon flux and energy resolution required for incisive measurements. This capability gap for measuring the essential observable

of an interacting electron system substantially limits our understanding of quantum materials. High repetition rate XFELs will bridge this capability gap and offer transformative capabilities; for both characterizing ground-state collective modes (energy and momentum dependence throughout the Brillouin zone), and for following their response to tailored excitations.

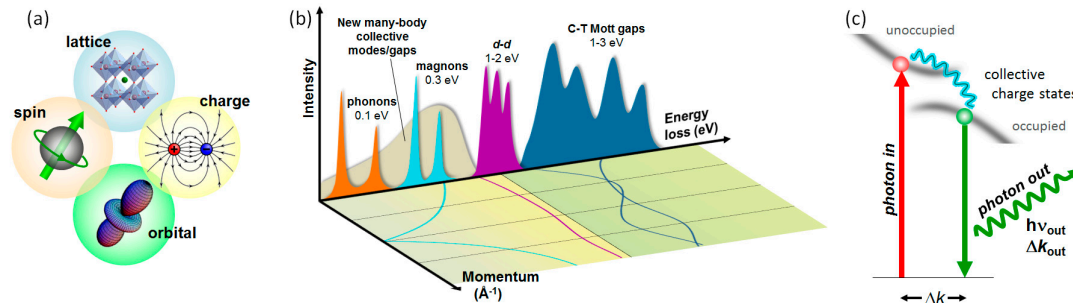


Figure 10. (a) Illustration of coupling between charge, spin, orbitals, and lattice. (b) Collective excitations that can be characterized by RIXS—including excitations within d-orbital manifolds (*d-d*) and charge-transfer excitations (C-T). Higher resolution is essential to reveal collective excitations at energy scales comparable to that of superconducting gap and pseudogap $\sim k_B T$ (< 25 meV) (image adapted from ref. [40]). (c) Resonant inelastic X-ray scattering (RIXS) probe of collective charge states.

Momentum-resolved resonant inelastic X-ray scattering (qRIXS) records the energy and momentum-transfer of scattered X-rays and is a powerful tool to map the energy-momentum dispersion of collective excitations [41]. This approach has been applied to characterize the energy-momentum dispersion of a range of collective excitations (such as magnons [42], paramagnons [43], triplons [44], two-spinons [45], phonons [46], orbitons [45] etc.) at a routinely available energy resolution of ~ 100 meV (resolving power $R \sim 10,000$). State-of-the-art RIXS instruments (e.g., ESRF ID32 [47], NSLS-II 2-ID SIX [48]) provide $R > 30,000$ to investigate collective excitations at energy scales comparable to the superconducting gap and pseudogap in unconventional high- T_c superconductors (< 50 meV). In spite of these advances, the inherent lack of longitudinal coherence (and therefore limited spectral flux, ph/s/meV) of synchrotron X-ray sources limits the ultimate scientific impact of qRIXS. High repetition rate seeded XFELs are anticipated to drive a qualitative advance in applications of qRIXS to quantum materials by providing nearly a 1000-fold increase in available X-ray spectral flux for studies at unprecedented resolution and sensitivity.

Beyond conventional qRIXS methods, *time-domain* approaches have tremendous potential to provide an important new perspective on collective excitations by selectively perturbing (or suppressing) one of the interacting degrees of freedom; e.g., by transient charge, spin, or vibrational excitation. Of particular interest is the stimulation of materials directly on the low-energy scales characteristic of the collective excitations (phonons, plasmons, magnons etc.). Ultrafast pulses spanning the visible-to-THz regimes are effective stimuli of coherent collective excitations and can transiently disrupt intertwined degrees of freedom. For example, recent studies have shown that broadband THz pulses can selectively couple to electronic order, and thereby transiently decouple charge and lattice modes [49]. Such approaches can also trigger phase transitions and create new phases that are inaccessible in thermal equilibrium [50–53], thus pointing the way toward control of quantum materials. For example, tailored ultrafast vibrational excitation has been shown to drive insulator-to-metal phase transitions in colossal magnetoresistive manganites [54], photo-induced superconductivity has been reported [50], and enhanced superconductivity is claimed to result from transiently-driven nonlinear lattice dynamics in YBCO [55] and K-doped C60 [56].

An unambiguous interpretation and characterization of these novel photo-induced phenomena is still lacking, but time- and momentum-resolved RIXS can provide much clearer insight. For example, time-resolved RIXS at the Cu L-edge can map the evolution of magnetic excitations and phonons in

time, energy, and momentum to provide a more complete microscopic picture about the transient photo-enhanced superconducting phase. The role of charge order in high- T_c superconductivity remains the subject of ongoing debate, and following the evolution of coexisting charge-stripe order through the transient phase will be incredibly informative. Time-resolved RIXS is applicable to a wide range of problems in quantum materials, such as the recently discovered branch of collective modes near the zone center in $\text{Nd}_{2x}\text{Ce}_x\text{CuO}_4$ and their putative connection to magnetic fluctuations [57].

3.4. Coherent X-ray Imaging at the Nanoscale—Heterogeneity and Dynamics

The ability to image individual non-identical particles in three dimensions at the atomic scale via coherent X-ray scattering remains one of the driving scientific visions for XFELs. This is based on the concept of “diffraction before destruction” whereby the interpretable scattering patterns are generated from individual X-ray pulses (of sufficient intensity and short duration) before X-ray damage effects degrade the achievable resolution [58]. Initial demonstration experiments and applications of single particle imaging methods at LCLS include single-shot coherent diffraction images of viruses [59], bacteriophages [60], organelles [61], and cyanobacteria [62].

Active ongoing research is refining the optimum conditions for single particle imaging. Biological samples are typically comprised of low- Z elements with low X-ray scattering cross-sections, thus yielding scattering snapshots with low signal-to-background ratios. Studies have suggested that the optimum photon energy for single particle imaging is in the tender X-ray range between 2 keV and 6 keV, which may represent the best compromise between scattering cross-section and resolution [63]. The assembly of complete data sets via single particle imaging is hampered by the low number of snapshots (at current low XFEL repetition rates), and further complicated by sample heterogeneity. In order to advance single particle imaging methods, LCLS has launched the single particle imaging (SPI) initiative to develop a roadmap towards the goal of imaging at 3 Å resolution [64]. The initiative consists of over 100 scientists from 20 international institutions and covers all aspects of SPI, from ultrafast X-ray induced damage processes to sample delivery and algorithm development. Recently, the SPI initiative reported scattering data from rice dwarf virus particles out to 3.0 Å (with scattering signals significantly above background) [65], and have pushed the state-of-the-art for 3D image reconstruction to below 10 nm [66].

LCLS-II presents some important opportunities for single particle imaging—particularly the possibility to image the dynamics of macromolecules and assemblies in near-native environments at room temperature. The high repetition rate of LCLS-II in the near-optimum tender X-ray range can potentially generate 10^8 to 10^{10} scattering snapshots per day, thereby driving a qualitative advance in our ability to map the conformational energy landscapes traversed by biological nanomachines. Cryogenic electron microscopy (cryo-EM) results demonstrate the potential to extract three-dimensional structure [67], conformational movies, and energy landscapes from ultralow-signal snapshots of biological complexes cryo-trapped in random orientations at statistically determined points in their work cycle [68]. In the low-signal regime, the number of available snapshots ultimately determines the information content of a conformational movie and the detail with which an energy landscape can be mapped.

Complementing single-particle imaging, fluctuation X-ray scattering (fSAXS) has emerged as a method bridging SPI and crystallography and is a potentially powerful approach for understanding protein interactions in native environments. fSAXS is a multi-particle scattering approach (based on a limited ensemble of particles) and is enabled by the combination of ultrafast X-ray pulses and high repetition rate [69–71]. It potentially provides ~100 times more information than conventional SAXS—sufficient for 3-D reconstruction. As an example, the dynamic fluctuations and conformational response of enzymes to active substrates or small molecules in physiological environments is central to their biological function, and current structural biology methods provide only limited insight. The repetition rate of LCLS-II combined with advanced microfluidic mixing liquid jets may open entirely new opportunities for investigating enzyme dynamics and their response to rapidly

introduced substrates. While rapid mixing enhances the population of transient intermediate states, they nevertheless constitute “rare events,” with their observation probability (and distinguishability from other states) determined by the reaction kinetics. High repetition rate XFELs will be essential to capture such rare events and characterize a distribution of transient intermediate structures.

4. Future Developments and Science Opportunities—LCLS-II-HE

The extension of high repetition rate XFELs to the hard X-ray regime is motivated by the scientific need for ultrafast atomic resolution at a high average power. LCLS-II-HE represents a significant next step in the ongoing revolution in X-ray lasers and is a natural extension to LCLS-II, based on known CW-SCRF accelerator technology and using existing LCLS infrastructure. LCLS-II-HE will extend operation of the high-repetition-rate LCLS-II beam into the critically important “hard X-ray” regime that has been used in more than 75% of LCLS experiments to date, providing a major advance in performance to the broadest cross-section of the user community. The energy reach of LCLS-II-HE (stretching from 5 keV to at least 13 keV and potentially up to 20 keV) will enable the study of atomic-scale dynamics with the penetrating power and pulse structure needed for *in situ* and *operando* studies of real-world materials, functioning assemblies, and biological systems. The projected performance of LCLS-II-HE in comparison to other X-ray sources is shown in Figure 11.

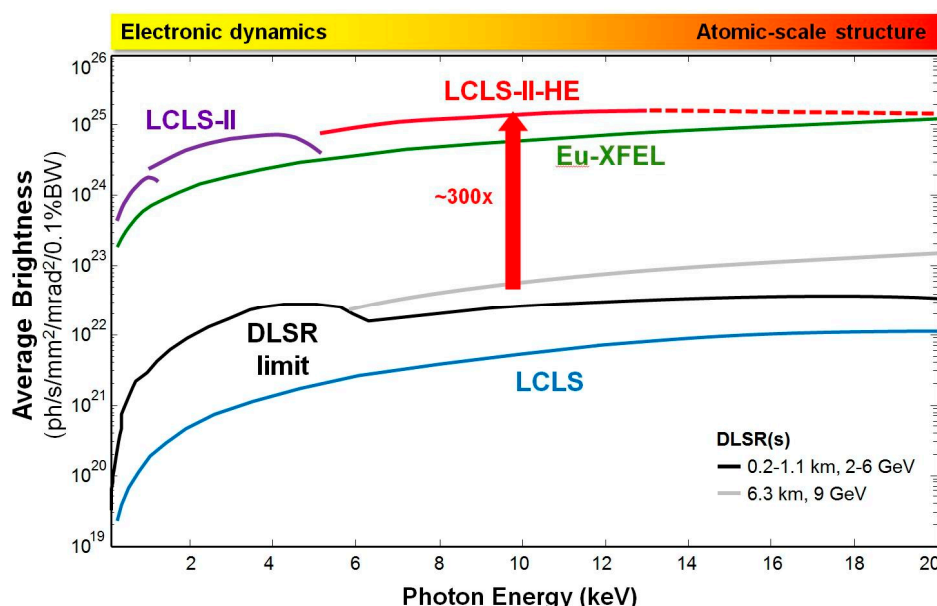


Figure 11. The performance of LCLS-II-HE will allow access to the ‘hard X-ray’ regime, providing atomic resolution capability, with an average brightness roughly 300 times the ultimate capability of a diffraction-limited storage ring (DLSR) [72]. Self-seeding will further increase the average brightness of the X-ray free-electron laser (XFEL) facilities by an additional factor of 20 to 50.

4.1. LCLS-II-HE Overview and Technical Capabilities

4.1.1. The Envisioned LCLS-II-HE Upgrade Will:

- Deliver two to three orders of magnitude of increase in average spectral brightness in the hard X-ray range beyond any proposed or envisioned diffraction-limited storage ring (DLSR) and exceed the anticipated performance of the European-XFEL.
- Provide temporal coherence for high-resolution spectroscopy near the Fourier transform limit with more than a 300-fold increase in average spectral flux (ph/s/meV) for high-resolution studies beyond any proposed or envisioned DLSR.

- Generate ultrafast hard X-ray pulses in a uniform (or programmable) time structure at a repetition rate of up to 1 MHz.
- Double the electron beam energy of the CW-SCRF linac to 8 GeV, thereby creating three independent accelerators within a single facility: (1) a new 8 GeV superconducting linac; (2) a separately tunable 3.6 GeV by-pass line for the LCLS-II instruments; and (3) the existing 15 GeV Cu-linac.

4.1.2. LCLS-II-HE Technical Capabilities

- **Access to the energy regime above 5 keV** for the analysis of key chemical elements and for atomic resolution. This regime encompasses Earth-abundant elements that are expected to comprise future photocatalysts for electricity and fuel production; it also accesses elements with strong spin-orbit coupling that are of significant interest for future quantum materials; and it reaches the biologically important selenium K-edge for phasing in protein crystallography.
- **High-repetition-rate, ultrafast hard X-rays** from LCLS-II-HE will reveal coupled atomic and electronic dynamics in unprecedented detail. Advanced X-ray techniques will simultaneously measure electronic structure and subtle nuclear displacements at the atomic scale, on fundamental timescales (femtosecond and longer), and in operating environments that require the penetrating capabilities of hard X-rays and the sensitivity provided by high repetition rate.
- **Temporal resolution:** LCLS-II-HE will deliver coherent X-rays on the fastest timescales, opening up experimental opportunities that were previously unattainable due to low signal-to-noise from LCLS (at 120 Hz) and that are simply not possible on non-laser sources. The performance of LCLS has progressed from initial pulse durations of 300 fs down to 5 fs, coupled to the capability for double pulses with independent control of energy, bandwidth, and timing. Ongoing development programs offer the potential for 0.5 fs pulses.
- **Temporal coherence:** Control over the XFEL bandwidth will be a major advance for high-resolution inelastic X-ray scattering and spectroscopy in the hard X-ray range (RIXS and IXS). The present scientific impact of RIXS and IXS is substantially limited by the available spectral flux (ph/s/meV) from temporally incoherent synchrotron sources. In the hard X-ray regime, LCLS-II-HE will provide more than a 300-fold increase in average spectral flux compared to synchrotron sources, opening new areas of science and exploiting high energy resolution and dynamics near the Fourier transform limit.
- **Spatial Coherence:** The high average coherent power of LCLS-II-HE in the hard X-ray range, with programmable pulses at high repetition rate, will enable studies of spontaneous ground-state fluctuations and heterogeneity at the atomic scale from μs (or longer) down to fundamental femtosecond timescales using powerful time-domain approaches such as X-ray photon correlation spectroscopy (XPCS). LCLS-II-HE capabilities will further provide a qualitative advance for understanding non-equilibrium dynamics and fluctuations via time-domain inelastic X-ray scattering (FT-IXS) and X-ray Fourier-transform spectroscopy approaches using Bragg crystal interferometers.
- **Structural dynamics and complete time sequences:** LCLS achieved early success in the determination of high-resolution structures of biological systems and nanoscale matter before the onset of damage. X-ray scattering with ultrashort pulses represents a step-change in the field of protein crystallography. An important scientific challenge is to understand function as determined by structural dynamics, at the atomic scale (requiring $\sim 1 \text{ \AA}$ resolution) and under operating conditions or in physiologically relevant environments (e.g., aqueous, room temperature). The potential of dynamic pump-probe structure studies has been demonstrated in model systems, but the much higher repetition rates of LCLS-II-HE are needed in order to extract complete time sequences from biologically relevant complexes. Here, small differential scattering signals that originate from dilute concentrations of active sites and low photolysis levels are essential in order to provide interpretable results.

- **Heterogeneous sample ensembles and rare events:** The high repetition rate and uniform time structure of LCLS-II-HE provide a transformational capability to collect 10^8 - 10^{10} scattering patterns (or spectra) per day with sample replacement between pulses. By exploiting revolutionary advances in data science (e.g., Bayesian analysis, pattern recognition, manifold maps, or machine-learning algorithms) it will be possible to characterize heterogeneous ensembles of particles or identify and extract new information about rare transient events from comprehensive data sets.

4.2. LCLS-I-HE Science Opportunities

LCLS-II-HE will enable precision measurements of structural dynamics on atomic spatial scales and fundamental timescales—providing detailed insight into the behavior of complex matter in real-world heterogeneous samples on fundamental scales of energy, time, and length. The solutions to many important challenges facing humanity, such as developing alternative sources of energy, mitigating environmental and climate problems, and delivering precision medical tools, depend on an improved understanding and control of matter.

We highlight seven broad classes of science for which LCLS-II-HE will uniquely address critical knowledge gaps.

4.2.1. Coupled Dynamics of Energy and Charge in Atoms and Molecules

Flows of energy and charge in molecules are the fundamental processes that drive chemical reactions and store or release energy. They are central to energy processes ranging from combustion to natural and man-made molecular systems that convert sunlight into fuels. Understanding and controlling these processes remains a fundamental science challenge, in large part because the movement of charge is closely coupled to subtle structural changes of the molecule, and conventional chemistry models are inadequate to fully describe this. Sharper experimental tools are needed to probe these processes—simultaneously at the atomic level and on natural (femtosecond) time scales. LCLS-II-HE will image dynamics at the atomic scale via hard X-ray scattering and coherent diffractive imaging (CDI) to reveal the coupled behavior of electrons and atoms with unprecedented clarity. The combination of hard X-rays with high peak power and high average power will enable new nonlinear spectroscopies that promise important new insights into reactive chemical flows in complex chemical environments such as combustion.

4.2.2. Catalysis, Photocatalysis, Environmental & Coordination Chemistry

A deeper understanding of the fundamental processes in catalysis, photocatalysis, and interfacial chemistry is essential for the directed design of new systems for chemical transformations, energy storage, and solar energy conversion that are efficient, chemically selective, robust, and based on Earth-abundant elements. LCLS-II-HE will reveal the critical (and often rare) transient events in these multistep processes, from light harvesting to charge separation, migration, and accumulation at catalytically active sites. Time-resolved, high-sensitivity, element-specific scattering and spectroscopy enabled by LCLS-II-HE will provide the first direct view of atomic-scale chemical dynamics at interfaces. The penetrating capability of hard X-rays will probe operating catalytic systems across multiple time and length scales. The unique LCLS-II-HE capability for simultaneous delivery of hard and soft X-ray pulses opens the possibility to follow chemical dynamics (via spectroscopy) concurrent with structural dynamics (substrate scattering) during heterogeneous catalysis. Time-resolved hard X-ray spectroscopy with high fidelity, enabled by LCLS-II-HE, will reveal the fine details of functioning biological catalysts (enzymes) and inform the design of artificial catalysts and networks with targeted functionality.

4.2.3. Imaging Biological Function and Dynamics

The combination of high spatial and time resolution with a high repetition rate will make LCLS-II-HE a revolutionary machine for many biological science fields. At high repetition rates,

serial femtosecond crystallography (SFX) will advance from successful demonstration experiments to address some of the most pressing challenges in structural biology for which only very limited sample volumes are available (e.g., human proteins); or only very small crystal sizes can be achieved ($<1 \mu\text{m}$); or where current structural information is significantly compromised by damage from conventional X-ray methods (e.g., redox effects in metalloproteins). In all of these cases, high throughput and near-physiological conditions of room temperature crystallography will be qualitative advances. X-ray energies spanning the Se K-edge (12.6 keV) will further enable *de novo* phasing and anomalous scattering. Time-resolved SFX and solution SAXS will advance from present few-time snapshots of model systems at high photolysis levels to full time sequences of molecular dynamics that are most relevant for biology. Hard X-rays and high repetition rates will further enable advanced crystallography methods that exploit diffuse scattering from imperfect crystals, as well as advanced solution scattering and single particle imaging methods to map sample heterogeneity and conformational dynamics in native environments.

4.2.4. Materials Heterogeneity, Fluctuations, and Dynamics

Heterogeneity and fluctuations of atoms and charge-carriers—spanning the range from the atomic scale to the mesoscale—underlie the performance and energy efficiency of functional materials and hierarchical devices. Conventional models of ideal materials often break down when trying to describe the properties that arise from these complex, non-equilibrium conditions. Yet, there exists an untapped potential to enhance material performance and create new functionality if we can achieve a much deeper insight into these statistical atomic-scale dynamics. Important examples include structural dynamics associated with ion transport in materials for energy storage devices and fuel cells; nanostructured materials for manipulating nonequilibrium thermal transport; two-dimensional materials and heterostructures with exotic properties that are strongly influenced by electron-phonon coupling, light-matter interactions, and subtle external stimuli; and perovskite photovoltaics where dynamic structural fluctuations influence power conversion efficiency. LCLS-II-HE will open an entirely new regime for time-domain coherent X-ray scattering of both statistical (e.g., XPCS) and triggered (pump-probe) dynamics with high average coherent power and penetrating capability for sensitive real-time, *in situ* probes of atomic-scale structure. This novel class of measurements will lead to new understanding of materials, and, ultimately, device performance, and will couple directly to both theory efforts and next-generation materials design initiatives.

4.2.5. Quantum Materials and Emergent Properties

There is an urgent technological need to understand and ultimately control the exotic quantum-based properties of new materials—ranging from superconductivity to ferroelectricity to magnetism. These properties emerge from the correlated interactions of the constituent matter components of charge, spin, and phonons, and are not well described by conventional band models that underpin present semiconductor technologies. A comprehensive description of the ground-state collective modes that appear at modest energies, 1 meV–100 meV, where modern X-ray sources and spectrometers lack the required combination of photon flux and energy resolution, is critical to understanding quantum materials. High-resolution hard X-ray scattering and spectroscopy at close to the Fourier limit will provide important new insights into the collective modes in *5d* transition metal oxides—where entirely new phenomena are now being discovered, owing to the combination of strong spin-orbit coupling and strong charge correlation. The ability to apply transient fields and forces (optical, THz, magnetic, pressure) with the time-structure of LCLS-II-HE will be a powerful approach for teasing apart intertwined ordering, and will be a step toward materials control that exploits coherent light-matter interaction. Deeper insight into the coupled electronic and atomic structure in quantum materials will be achieved via simultaneous atomic-resolution scattering and bulk-sensitive photoemission enabled by LCLS-II-HE hard X-rays and high repetition rate.

4.2.6. Materials in Extreme Environments

LCLS-II-HE studies of extreme materials will be important for fusion and fission material applications and could lead to important insights into planetary physics and geoscience. The unique combination of capabilities from LCLS-II-HE will enable the high-resolution spectroscopic and structural characterization of matter in extreme states that is far beyond what is achievable today. High peak brightness combined with high repetition rates and high X-ray energies are required to (i) penetrate dynamically heated dense targets and diamond anvil cells (DAC); (ii) achieve high signal-to-noise data above the self-emission bremsstrahlung background; (iii) probe large momentum transfers on atomic scales to reveal structure and material phases; and (iv) measure inelastic X-ray scattering with sufficient energy resolution and sensitivity to determine the physical properties of materials.

4.2.7. Nonlinear X-ray Matter Interactions

A few seminal experiments on the first generation of X-ray free-electron lasers, LCLS and SACLA, have demonstrated new fundamental nonlinear hard X-ray-matter interactions, including phase-matched sum frequency generation, second harmonic generation, and two-photon Compton scattering. While nonlinear X-ray optics is still in the discovery-based science phase, advances in our understanding of these fundamental interactions will lead to powerful new tools for atomic and molecular physics, chemistry, materials science, and biology via measurement of valence charge density at atomic resolution and on the attosecond-to-femtosecond timescale of electron motion. The combination of high repetition rate and high peak intensity pulses from LCLS-II-HE will enable high-sensitivity measurements that exploit subtle nonlinear effects. This will transform the nonlinear X-ray optics field from demonstration experiments to real measurements that utilize the nonlinear interactions of “photon-in, photon-out” to simultaneously access transient spectroscopic and structural information from real materials.

5. Conclusions

Recent accomplishments from LCLS in the areas of atomic, molecular, and optical science; chemistry; condensed matter physics; matter in extreme conditions; and biology are just a few of the many examples illustrating the ongoing rapid development of XFEL science. At the same time, important new science opportunities are driving the development of a new generation of XFELs that will exploit continuous-wave superconducting accelerator technology to provide ultrafast X-ray pulses at a high repetition rate (~MHz) in a uniform or programmable time structure. The LCLS upgrade project (LCLS-II) will provide ultrafast X-rays in the 0.25–5.0 keV range at repetition rates up to 1 MHz with two independent XFELs based on adjustable-gap undulators: 0.25–1.25 keV soft X-ray undulator (SXU) and 1–5 keV hard X-ray undulator (HXU), with first-light projected for 2020 [4]. In this paper, we have highlighted a few of the important new science opportunities enabled by such a facility in the areas of (1) fundamental charge and energy flow in molecular complexes; (2) photo-catalysis and coordination chemistry; (3) quantum materials; and (4) coherent imaging at the nanoscale. A second phase upgrade is envisioned to extend the X-ray energy reach to beyond 13 keV (<1 Å) at high repetition rate by doubling the CW-SCRF linac energy to 8 GeV. This is motivated by compelling new science of structural dynamics at the atomic scale.

Acknowledgments: The Linac Coherent Light Source (LCLS) at the SLAC National Accelerator Laboratory is an Office of Science User Facility operated for the U.S. Department of Energy Office of Science by Stanford University. This work was supported by the U.S. Department of Energy, Office of Science, Basic Energy Sciences under Contract No. DEAC02-76SF00515.

Conflicts of Interest: The authors declare no conflict of interest.

References

1. Ayvazyan, V.; Baboi, N.; Bähr, J.; Balandin, V.; Beutner, B.; Brandt, A.; Bohnet, I.; Bolzmann, A.; Brinkmann, R.; Brovko, O.I.; et al. First operation of a free-electron laser generating gw power radiation at 32 nm wavelength. *Eur. Phys. J. D* **2006**, *37*, 297–303. [[CrossRef](#)]
2. Ishikawa, T.; Aoyagi, H.; Asaka, T.; Asano, Y.; Azumi, N.; Bizen, T.; Ego, H.; Fukami, K.; Fukui, T.; Furukawa, Y.; et al. A compact X-ray free-electron laser emitting in the sub-angstrom region. *Nat. Photonics* **2012**, *6*, 540–544. [[CrossRef](#)]
3. Bostedt, C.; Boutet, S.; Fritz, D.M.; Huang, Z.; Lee, H.J.; Lemke, H.T.; Robert, A.; Schlotter, W.F.; Turner, J.J.; Williams, G.J. Linac coherent light source: The first five years. *Rev. Mod. Phys.* **2016**, *88*, 015007. [[CrossRef](#)]
4. SLAC National Accelerator Laboratory. *Linac Coherent Light Source II (LCLS-II) Project Final Design Report—LCLSII-1.1-dr-0251-r0*; SLAC National Accelerator Laboratory: Menlo Park, CA, USA, 2015.
5. Minitti, M.P.; Budarz, J.M.; Kirrander, A.; Robinson, J.S.; Ratner, D.; Lane, T.J.; Zhu, D.; Glowonia, J.M.; Kozina, M.; Lemke, H.T.; et al. Imaging molecular motion: Femtosecond X-ray scattering of an electrocyclic chemical reaction. *Phys. Rev. Lett.* **2015**, *114*, 255501. [[CrossRef](#)] [[PubMed](#)]
6. Woodward, R.B.; Hoffmann, R. The conservation of orbital symmetry. *Angew. Chem. Int.* **1969**, *8*, 781–853. [[CrossRef](#)]
7. Wernet, P.; Kunnus, K.; Josefsson, I.; Rajkovic, I.; Quevedo, W.; Beye, M.; Schreck, S.; Grubel, S.; Scholz, M.; Nordlund, D.; et al. Orbital-specific mapping of the ligand exchange dynamics of Fe(CO)₅ in solution. *Nature* **2015**, *520*, 78–81. [[CrossRef](#)] [[PubMed](#)]
8. Jiang, M.P.; Trigo, M.; Savić, I.; Fahy, S.; Murray, É.D.; Bray, C.; Clark, J.; Henighan, T.; Kozina, M.; Chollet, M.; et al. The origin of incipient ferroelectricity in lead telluride. *Nat. Commun.* **2016**, *7*, 12291. [[CrossRef](#)] [[PubMed](#)]
9. Trigo, M.; Fuchs, M.; Chen, J.; Jiang, M.P.; Cammarata, M.; Fahy, S.; Fritz, D.M.; Gaffney, K.; Ghimire, S.; Higginbotham, A.; et al. Fourier-transform inelastic X-ray scattering from time- and momentum-dependent phonon-phonon correlations. *Nat. Phys.* **2013**, *9*, 790–794. [[CrossRef](#)]
10. Zhu, D.; Robert, A.; Henighan, T.; Lemke, H.T.; Chollet, M.; Glowonia, J.M.; Reis, D.A.; Trigo, M. Phonon spectroscopy with sub-meV resolution by femtosecond X-ray diffuse scattering. *Phys. Rev. B* **2015**, *92*, 054303. [[CrossRef](#)]
11. Gerber, S.; Jang, H.; Nojiri, H.; Matsuzawa, S.; Yasumura, H.; Bonn, D.A.; Liang, R.; Hardy, W.N.; Islam, Z.; Mehta, A.; et al. Three-dimensional charge density wave order in YBa₂Cu₃O_{6.67} at high magnetic fields. *Science* **2015**, *350*, 949–952. [[CrossRef](#)] [[PubMed](#)]
12. McMahon, M.; Nelmes, R. Incommensurate crystal structures in the elements at high pressure. *Z. Kristallogr.—Cryst. Mater.* **2004**, *219*, 742. [[CrossRef](#)]
13. Briggs, R.; Gorman, M.G.; Coleman, A.L.; McWilliams, R.S.; McBride, E.E.; McGonegle, D.; Wark, J.S.; Peacock, L.; Rothman, S.; Macleod, S.G.; et al. Ultrafast X-ray diffraction studies of the phase transitions and equation of state of scandium shock compressed to 82 gpa. *Phys. Rev. Lett.* **2017**, *118*, 025501. [[CrossRef](#)] [[PubMed](#)]
14. Fujihisa, H.; Akahama, Y.; Kawamura, H.; Gotoh, Y.; Yamawaki, H.; Sakashita, M.; Takeya, S.; Honda, K. Incommensurate composite crystal structure of scandium-ii. *Phys. Rev. B* **2005**, *72*, 132103. [[CrossRef](#)]
15. Martin-Garcia, J.M.; Conrad, C.E.; Coe, J.; Roy-Chowdhury, S.; Fromme, P. Serial femtosecond crystallography: A revolution in structural biology. *Arch. Biochem. Biophys.* **2016**, *602*, 32–47. [[CrossRef](#)] [[PubMed](#)]
16. Levantino, M.; Yorke, B.A.; Monteiro, D.C.F.; Cammarata, M.; Pearson, A.R. Using synchrotrons and xfel for time-resolved X-ray crystallography and solution scattering experiments on biomolecules. *Curr. Opin. Struct. Biol.* **2015**, *35*, 41–48. [[CrossRef](#)] [[PubMed](#)]
17. Schlichting, I. Serial femtosecond crystallography: The first five years. *IUCr* **2015**, *2*, 246–255. [[CrossRef](#)] [[PubMed](#)]
18. Stagno, J.R.; Liu, Y.; Bhandari, Y.R.; Conrad, C.E.; Panja, S.; Swain, M.; Fan, L.; Nelson, G.; Li, C.; Wendel, D.R.; et al. Structures of riboswitch rna reaction states by mix-and-inject xfel serial crystallography. *Nature* **2017**, *541*, 242–246. [[CrossRef](#)] [[PubMed](#)]

19. Young, I.D.; Ibrahim, M.; Chatterjee, R.; Gul, S.; Fuller, F.D.; Koroidov, S.; Brewster, A.S.; Tran, R.; Alonso-Mori, R.; Kroll, T.; et al. Structure of photosystem ii and substrate binding at room temperature. *Nature* **2016**, *540*, 453–457. [[CrossRef](#)] [[PubMed](#)]
20. Emma, P.; Bane, K.; Cornacchia, M.; Huang, Z.; Schlarb, H.; Stupakov, G.; Walz, D. Femtosecond and subfemtosecond X-ray pulses from a self-amplified spontaneous-emission-based free-electron laser. *Phys. Rev. Lett.* **2004**, *92*, 074801. [[CrossRef](#)] [[PubMed](#)]
21. Ding, Y.; Brachmann, A.; Decker, F.J.; Dowell, D.; Emma, P.; Frisch, J.; Gilevich, S.; Hays, G.; Hering, P.; Huang, Z.; et al. Measurements and simulations of ultralow emittance and ultrashort electron beams in the linac coherent light source. *Phys. Rev. Lett.* **2009**, *102*, 254801. [[CrossRef](#)] [[PubMed](#)]
22. Amann, J.; Berg, W.; Blank, V.; Decker, F.-J.; Ding, Y.; Emma, P.; Feng, Y.; Frisch, J.; Fritz, D.; Hastings, J.; et al. Demonstration of self-seeding in a hard-X-ray free-electron laser. *Nat. Photonics* **2012**, *6*, 693–698. [[CrossRef](#)]
23. Ratner, D.; Abela, R.; Amann, J.; Behrens, C.; Bohler, D.; Bouchard, G.; Bostedt, C.; Boyes, M.; Chow, K.; Cocco, D.; et al. Experimental demonstration of a soft X-ray self-seeded free-electron laser. *Phys. Rev. Lett.* **2015**, *114*, 054801. [[CrossRef](#)] [[PubMed](#)]
24. Behrens, C.; Decker, F.J.; Ding, Y.; Dolgashev, V.A.; Frisch, J.; Huang, Z.; Krejcik, P.; Loos, H.; Lutman, A.; Maxwell, T.J.; et al. Few-femtosecond time-resolved measurements of X-ray free-electron lasers. *Nat. Commun.* **2014**, *5*, 3762. [[CrossRef](#)] [[PubMed](#)]
25. Lutman, A.A.; Maxwell, T.J.; MacArthur, J.P.; Guetg, M.W.; Berrah, N.; Coffee, R.N.; Ding, Y.; Huang, Z.; Marinelli, A.; Moeller, S.; et al. Fresh-slice multicolour X-ray free-electron lasers. *Nat. Photonics* **2016**, *10*, 745–750. [[CrossRef](#)]
26. Schlichting, I.; White, W.E.; Yabashi, M. Journal of synchrotron radiation: Special issue on X-ray free-electron lasers. *J. Synchrotron Radiat.* **2016**, *22*, 471–866. [[CrossRef](#)] [[PubMed](#)]
27. SLAC National Accelerator Laboratory. *Menlo Park New Science Opportunities Enabled by LCLS-II X-ray Lasers*; SLAC-R-1053; SLAC National Accelerator Laboratory: Menlo Park, CA, USA, 2015.
28. Worth, G.A.; Cederbaum, L.S. Beyond born-oppenheimer: Molecular dynamics through a conical intersection. *Annu. Rev. Phys. Chem.* **2004**, *55*, 127–158. [[CrossRef](#)] [[PubMed](#)]
29. Scholes, G.D.; Fleming, G.R.; Chen, L.X.; Aspuru-Guzik, A.; Buchleitner, A.; Coker, D.F.; Engel, G.S.; van Grondelle, R.; Ishizaki, A.; Jonas, D.M.; et al. Using coherence to enhance function in chemical and biophysical systems. *Nature* **2017**, *543*, 647–656. [[CrossRef](#)] [[PubMed](#)]
30. Dörner, R.; Mergel, V.; Jagutzki, O.; Spielberger, L.; Ullrich, J.; Moshhammer, R.; Schmidt-Böcking, H. Cold target recoil ion momentum spectroscopy: A ‘momentum microscope’ to view atomic collision dynamics. *Phys. Rep.* **2000**, *330*, 95–192. [[CrossRef](#)]
31. Landers, A.; Weber, T.; Ali, I.; Cassimi, A.; Hattass, M.; Jagutzki, O.; Nauert, A.; Osipov, T.; Staudte, A.; Prior, M.H.; et al. Photoelectron diffraction mapping: Molecules illuminated from within. *Phys. Rev. Lett.* **2001**, *87*, 013002. [[CrossRef](#)] [[PubMed](#)]
32. Ullrich, J.; Moshhammer, R.; Dorn, A.; Dörner, R.; Schmidt, L.P.H.; Schmidt-Böcking, H. Recoil-ion and electron momentum spectroscopy: Reaction-microscopes. *Rep. Prog. Phys.* **2003**, *66*, 1463. [[CrossRef](#)]
33. Erk, B.; Boll, R.; Trippel, S.; Anielski, D.; Foucar, L.; Rudek, B.; Epp, S.W.; Coffee, R.; Carron, S.; Schorb, S.; et al. Imaging charge transfer in iodomethane upon X-ray photoabsorption. *Science* **2014**, *345*, 288–291. [[CrossRef](#)] [[PubMed](#)]
34. Rudenko, A.; Rolles, D. Time-resolved studies with FELs. *J. Electron Spectrosc. Relat. Phenom.* **2015**, *204*, 228–236. [[CrossRef](#)]
35. Zeller, S.; Kunitski, M.; Voigtsberger, J.; Kalinin, A.; Schottelius, A.; Schober, C.; Waitz, M.; Sann, H.; Hartung, A.; Bauer, T.; et al. Imaging the He₂ quantum halo state using a free electron laser. *Proc. Natl. Acad. Sci. USA* **2016**, *113*, 14651–14655. [[CrossRef](#)] [[PubMed](#)]
36. Schnorr, K.; Senftleben, A.; Kurka, M.; Rudenko, A.; Foucar, L.; Schmid, G.; Broska, A.; Pfeifer, T.; Meyer, K.; Anielski, D.; et al. Time-resolved measurement of interatomic coulombic decay in Ne₂. *Phys. Rev. Lett.* **2013**, *111*, 093402. [[CrossRef](#)] [[PubMed](#)]
37. Schnorr, K.; Senftleben, A.; Kurka, M.; Rudenko, A.; Schmid, G.; Pfeifer, T.; Meyer, K.; Kübel, M.; Kling, M.F.; Jiang, Y.H.; et al. Electron rearrangement dynamics in dissociating i₂ⁿ⁺ molecules accessed by extreme ultraviolet pump-probe experiments. *Phys. Rev. Lett.* **2014**, *113*, 073001. [[CrossRef](#)] [[PubMed](#)]

38. McFarland, B.K.; Farrell, J.P.; Miyabe, S.; Tarantelli, F.; Aguilar, A.; Berrah, N.; Bostedt, C.; Bozek, J.D.; Bucksbaum, P.H.; Castagna, J.C.; et al. Ultrafast X-ray auger probing of photoexcited molecular dynamics. *Nat. Commun.* **2014**, *5*, 4235. [[CrossRef](#)] [[PubMed](#)]
39. Pitzer, M.; Kunitski, M.; Johnson, A.S.; Jahnke, T.; Sann, H.; Sturm, F.; Schmidt, L.P.H.; Schmidt-Bocking, H.; Dorner, R.; Stohner, J.; et al. Direct determination of absolute molecular stereochemistry in gas phase by coulomb explosion imaging. *Science* **2013**, *341*, 1096–1100. [[CrossRef](#)] [[PubMed](#)]
40. Zhu, Y.; Durr, H. The future of electron microscopy. *Phys. Today* **2015**, *68*, 32. [[CrossRef](#)]
41. Ament, L.J.P.; van Veenendaal, M.; Devereaux, T.P.; Hill, J.P.; van den Brink, J. Resonant inelastic X-ray scattering studies of elementary excitations. *Rev. Mod. Phys.* **2011**, *83*, 705–767. [[CrossRef](#)]
42. Guarise, M.; Dalla Piazza, B.; Moretti Sala, M.; Ghiringhelli, G.; Braicovich, L.; Berger, H.; Hancock, J.N.; van der Marel, D.; Schmitt, T.; Strocov, V.N.; et al. Measurement of magnetic excitations in the two-dimensional antiferromagnetic $\text{Sr}_2\text{CuO}_2\text{Cl}_2$ insulator using resonant X-ray scattering: Evidence for extended interactions. *Phys. Rev. Lett.* **2010**, *105*, 157006. [[CrossRef](#)] [[PubMed](#)]
43. Le Tacon, M.; Ghiringhelli, G.; Chaloupka, J.; Sala, M.M.; Hinkov, V.; Haverkort, M.W.; Minola, M.; Bakr, M.; Zhou, K.J.; Blanco-Canosa, S.; et al. Intense paramagnon excitations in a large family of high-temperature superconductors. *Nat. Phys.* **2011**, *7*, 725–730. [[CrossRef](#)]
44. Schlappa, J.; Schmitt, T.; Vernay, F.; Strocov, V.N.; Ilakovac, V.; Thielemann, B.; Rønnow, H.M.; Vanishri, S.; Piazzalunga, A.; Wang, X.; et al. Collective magnetic excitations in the spin ladder $\text{Sr}_{14}\text{Cu}_{24}\text{O}_{41}$ measured using high-resolution resonant inelastic X-ray scattering. *Phys. Rev. Lett.* **2009**, *103*, 047401. [[CrossRef](#)] [[PubMed](#)]
45. Schlappa, J.; Wohlfeld, K.; Zhou, K.J.; Mourigal, M.; Haverkort, M.W.; Strocov, V.N.; Hozoi, L.; Monney, C.; Nishimoto, S.; Singh, S.; et al. Spin-orbital separation in the quasi-one-dimensional mott insulator Sr_2CuO_3 . *Nature* **2012**, *485*, 82–85. [[CrossRef](#)] [[PubMed](#)]
46. Lee, W.S.; Johnston, S.; Moritz, B.; Lee, J.; Yi, M.; Zhou, K.J.; Schmitt, T.; Patthey, L.; Strocov, V.; Kudo, K.; et al. Role of lattice coupling in establishing electronic and magnetic properties in quasi-one-dimensional cuprates. *Phys. Rev. Lett.* **2013**, *110*, 265502. [[CrossRef](#)] [[PubMed](#)]
47. ESRF ID-32 Soft X-ray Spectroscopy Beamline. Available online: <http://www.esrf.eu/ID32> (accessed on 14 August 2017).
48. NSLS-II Soft Inelastic X-ray Scattering (SIX) Beamline (2-ID). Available online: <https://www.bnl.gov/ps/beamlines/beamline.php?b=SIX> (accessed on 14 August 2017).
49. Porer, M.; Leierseder, U.; Ménard, J.M.; Dachraoui, H.; Mouchliadis, L.; Perakis, I.E.; Heinzmann, U.; Demsar, J.; Rossnagel, K.; Huber, R. Non-thermal separation of electronic and structural orders in a persisting charge density wave. *Nat. Mater.* **2014**, *13*, 857–861. [[CrossRef](#)] [[PubMed](#)]
50. Fausti, D.; Tobey, R.I.; Dean, N.; Kaiser, S.; Dienst, A.; Hoffmann, M.C.; Pyon, S.; Takayama, T.; Takagi, H.; Cavalleri, A. Light-induced superconductivity in a stripe-ordered cuprate. *Science* **2011**, *331*, 189–191. [[CrossRef](#)] [[PubMed](#)]
51. Schmitt, F.; Kirchmann, P.S.; Bovensiepen, U.; Moore, R.G.; Rettig, L.; Krenz, M.; Chu, J.-H.; Ru, N.; Perfetti, L.; Lu, D.H.; et al. Transient electronic structure and melting of a charge density wave in TbTe_3 . *Science* **2008**, *321*, 1649–1652. [[CrossRef](#)] [[PubMed](#)]
52. Hinton, J.P.; Koralek, J.D.; Lu, Y.M.; Vishwanath, A.; Orenstein, J.; Bonn, D.A.; Hardy, W.N.; Liang, R.X. New collective mode in $\text{YBa}_2\text{Cu}_3\text{O}_{6+x}$ observed by time-domain reflectometry. *Phys. Rev. B* **2013**, *88*, 060508. [[CrossRef](#)]
53. Stojchevska, L.; Vaskivskyi, I.; Mertelj, T.; Kusar, P.; Svetin, D.; Brazovskii, S.; Mihailovic, D. Ultrafast switching to a stable hidden quantum state in an electronic crystal. *Science* **2014**, *344*, 177–180. [[CrossRef](#)] [[PubMed](#)]
54. Rini, M.; Tobey, R.; Dean, N.; Itatani, J.; Tomioka, Y.; Tokura, Y.; Schoenlein, R.W.; Cavalleri, A. Control of the electronic phase of a manganite by mode-selective vibrational excitation. *Nature* **2007**, *449*, 72–74. [[CrossRef](#)] [[PubMed](#)]
55. Mankowsky, R.; Subedi, A.; Forst, M.; Mariager, S.O.; Chollet, M.; Lemke, H.T.; Robinson, J.S.; Glownia, J.M.; Miniti, M.P.; Frano, A.; et al. Nonlinear lattice dynamics as a basis for enhanced superconductivity in $\text{YBa}_2\text{Cu}_3\text{O}_{6.5}$. *Nature* **2014**, *516*, 71–73. [[CrossRef](#)] [[PubMed](#)]

56. Mitrano, M.; Cantaluppi, A.; Nicoletti, D.; Kaiser, S.; Perucchi, A.; Lupi, S.; Di Pietro, P.; Pontiroli, D.; Riccò, M.; Clark, S.R.; et al. Possible light-induced superconductivity in K_3C_{60} at high temperature. *Nature* **2016**, *530*, 461–464. [[CrossRef](#)] [[PubMed](#)]
57. Lee, W.S.; Lee, J.J.; Nowadnick, E.A.; Gerber, S.; Tabis, W.; Huang, S.W.; Strocov, V.N.; Motoyama, E.M.; Yu, G.; Moritz, B.; et al. Asymmetry of collective excitations in electron- and hole-doped cuprate superconductors. *Nat. Phys.* **2014**, *10*, 883–889. [[CrossRef](#)]
58. Neutze, R.; Wouts, R.; Spoel, D.v.d.; Weckert, E.; Hajdu, J. Potential for biomolecular imaging with femtosecond X-ray pulses. *Nature* **2000**, *406*, 752–757. [[CrossRef](#)] [[PubMed](#)]
59. Seibert, M.M.; Ekeberg, T.; Maia, F.R.N.C.; Svenda, M.; Andreasson, J.; Jonsson, O.; Odic, D.; Iwan, B.; Rocker, A.; Westphal, D.; et al. Single mimivirus particles intercepted and imaged with an X-ray laser. *Nature* **2011**, *470*, 78–81. [[CrossRef](#)] [[PubMed](#)]
60. Kassemeyer, S.; Steinbrener, J.; Lomb, L.; Hartmann, E.; Aquila, A.; Barty, A.; Martin, A.V.; Hampton, C.Y.; Bajt, S.A.; Barthelmess, M.; et al. Femtosecond free-electron laser X-ray diffraction data sets for algorithm development. *Opt. Express* **2012**, *20*, 4149–4158. [[CrossRef](#)] [[PubMed](#)]
61. Hantke, M.F.; Hasse, D.; Maia, F.R.N.C.; Ekeberg, T.; John, K.; Svenda, M.; Loh, N.D.; Martin, A.V.; Timneanu, N.; Larsson, D.S.D.; et al. High-throughput imaging of heterogeneous cell organelles with an X-ray laser. *Nat. Photonics* **2014**, *8*, 943–949. [[CrossRef](#)]
62. Van der Schot, G.; Svenda, M.; Maia, F.R.N.C.; Hantke, M.; DePonte, D.P.; Seibert, M.M.; Aquila, A.; Schulz, J.; Kirian, R.; Liang, M.; et al. Imaging single cells in a beam of live cyanobacteria with an X-ray laser. *Nat. Commun.* **2015**, *6*, 5704. [[CrossRef](#)] [[PubMed](#)]
63. Bergh, M.; Huldtd, G.; Timneanu, N.; Maia, F.R.N.C.; Hajdu, J. Feasibility of imaging living cells at subnanometer resolutions by ultrafast X-ray diffraction. *Q. Rev. Biophys.* **2008**, *41*, 181–204. [[CrossRef](#)] [[PubMed](#)]
64. Aquila, A.; Barty, A.; Bostedt, C.; Boutet, S.; Carini, G.; dePonte, D.; Drell, P.; Doniach, S.; Downing, K.H.; Earnest, T.; et al. The linac coherent light source single particle imaging road map. *Struct. Dyn.* **2015**, *2*, 041701. [[CrossRef](#)] [[PubMed](#)]
65. Munke, A.; Andreasson, J.; Aquila, A.; Awel, S.; Ayyer, K.; Barty, A.; Bean, R.J.; Berntsen, P.; Bielecki, J.; Boutet, S.; et al. Coherent diffraction of single rice dwarf virus particles using hard X-rays at the linac coherent light source. *Sci. Data* **2016**, *3*, 160064. [[CrossRef](#)] [[PubMed](#)]
66. Hosseinizadeh, A.; Mashayekhi, G.; Copperman, J.; Schwander, P.; Dashti, A.; Sepehr, R.; Fung, R.; Schmidt, M.; Yoon, C.H.; Hogue, B.G.; et al. Conformational landscape of a virus by single-particle X-ray scattering. *Nat. Methods* **2017**. [[CrossRef](#)] [[PubMed](#)]
67. Frank, J. *Three-Dimensional Electron Microscopy of Macromolecular Assemblies*, 2nd ed.; Oxford University Press: New York, NY, USA, 2006.
68. Dashti, A.; Schwander, P.; Langlois, R.; Fung, R.; Li, W.; Hosseinizadeh, A.; Liao, H.Y.; Pallesen, J.; Sharma, G.; Stupina, V.A.; et al. Trajectories of the ribosome as a brownian nanomachine. *Proc. Natl. Acad. Sci. USA* **2014**, *111*, 17492–17497. [[CrossRef](#)] [[PubMed](#)]
69. Kam, Z. Determination of macromolecular structure in solution by spatial correlation of scattering fluctuations. *Macromolecules* **1977**, *10*, 927–934. [[CrossRef](#)]
70. Kam, Z.; Koch, M.H.; Bordas, J. Fluctuation X-ray scattering from biological particles in frozen solution by using synchrotron radiation. *Proc. Natl. Acad. Sci. USA* **1981**, *78*, 3559–3562. [[CrossRef](#)] [[PubMed](#)]
71. Saldin, D.K.; Shneerson, V.L.; Howells, M.R.; Marchesini, S.; Chapman, H.N.; Bogan, M.; Shapiro, D.; Kirian, R.A.; Weierstall, U.; Schmidt, K.E.; et al. Structure of a single particle from scattering by many particles randomly oriented about an axis: Toward structure solution without crystallization. *New J. Phys.* **2010**, *12*, 14. [[CrossRef](#)]
72. Borland, M.; Advanced Photon Source (APS), Argonne National Laboratory; Steier, C.; ALS. Personal communication: DLSR contributions, 2016.

